JEAS

JOURNAL OF ENGINEERING AND APPLIED SCIENCES

Journal of Engineering and Applied Sciences, Volume 19, Number 1, December 2021, 519 - 532

Intelligence Modelling of Tensile Strength Response of Mild Steel Plate Weldments Obtained Using Gas Tungsten Arc Welding Process

M.K. Achike[1*], P. C. Onyechi[2] and C. C. Ihueze[3]

[1*]Department of Metalwork Technology Education, Federal College of Education (Technical), Umunze, Nigeria.

[2,3]Department of Industrial/Production Engineering, Nnamdi Azikiwe University, Awka, Nigeria.

[*]CorrespondingAuthor's E-mail: achike4christ07@yahoo.com

Abstract

This paper aimed at optimizing the process parameters and intelligence modelling of tensile strength response of mild steel plate weldments obtained using Gas Tungsten Arc Welding (GTAW) process. Taguchi robust design and intelligent modelling techniques (artificial neural networks and extreme learning machine) were used to model the experimental results. In designing the experimental runs for this research, Taguchi design of experiment which consists of four controllable parameters at 3-levels of design for which we chose the L_9 orthogonal array was used. Signal- to- noise ratio (S/N) which is an important quality characteristics of Taguchi method employed the larger-the-better criterion for tensile strength response. Minitab 16 Software was used for analysis of signal-to-noise ratio and ANOVA was used to validate the results at 95% confidence level. The ANN and ELM model simulations were carried out in the MATLAB 2018a environment at three different hidden neural nodes of 10, 20 and 30 neurons for the twenty (20) experimental runs. ELM algorithm showed a very good model fit at 30 neural nodes with a coefficient of determination (R^2) value of 98.4% which is far better than that of ANN algorithm and regression model which has R^2 values of 94.1% and 92.8% respectively. By comparing the experimental results with those obtained using ANN and ELM models, it can be concluded that the ELM model is more efficient in predicting tensile strength of mild steel plate weldments.

Keywords: Gas Tungsten Arc Welding, Tensile Strength, Taguchi Method, ANN, ELM

1. Introduction

The American Welding Society (2004) defined welding as a localized coalescence of metals or non-metals produced by either heating of the materials to a suitable temperature with or without the application of pressure or by the application of pressure alone with or without the use of a filler material. It is a process that involves localized heat generation from a moving heat source. The welded structures are heated rapidly up to the melting temperature, and followed by rapid cooling which causes micro-structural and property alterations (Devaraju 2015). Arc welding processes use a welding power supply to create and maintain an electric arc between an electrode and the base material to melt metals at the welding point.

Gas Tungsten Arc Welding (GTAW) uses a non-consumable tungsten electrode to heat and melt the workpiece and a separate filler metal with an inert shielding gas to protect the arc. A GTAW process set utilizes suitable power source, a cylinder of inert gas, a welding torch having connections of cable for current, tubing for shielding gas supply, and tubing for water for cooling the torch. The shape of torch is characteristic, having a cap at the back end to protect the rather long tungsten electrode against accidental breakage. Filler metal can be fed and molten puddle is shielded from the atmosphere with an inert gas supply feeding from the torch cup.

GTAW process welds different types of metals and alloys (carbon steel, stainless steel, nickel steels, copper, brass, bronze, etc). Unlike metals can be welded to each other like mild steel to stainless steel, brass to copper, etc. Heat-affected zone (weak area for failure of sound weld) is very low. Filler metal need not pass through the superheated electric arc. It requires no clean up after welding due to absence of slag or spatter (Jain 2013).

Machine Learning (ML) is a branch of Artificial Intelligence (AI) which focuses on the use of data and algorithms to imitate the way that humans learn, gradually improving its accuracy (Dietterich 1990; Okafor, Okafor & Ikebudu 2021). Machine learning algorithms build a model based on sample data known as "training data" in order to make predictions or decisions without being explicitly programmed to do so. Artificial Neural Networks (ANN) and Extreme Learning Machine (ELM) are the two main classes of non-symbolic machine learning tools applied in this research.

ANN is an interconnected assembly of simple processing elements, units or nodes whose functionality is loosely based on the animal neuron. The processing ability of the network is stored in the inter-unit connection or weights, obtained by a process of adaptation to or learning from a set of training patterns (Gurney 1997). ANN can be 'trained' to model relationships between input and output parameters from examples of the known inputs and their corresponding outputs. In the training process, a set of examples of input-output pairs are passed through the model and the weights are adjusted in order to minimize error between the answers from the network and the desired outputs (Reed & Marks, 1998). This weight alteration procedure is controlled by the learning algorithm. These inputs and outputs are presented to the network using neurons located in input and output layers respectively as shown in figure 1.

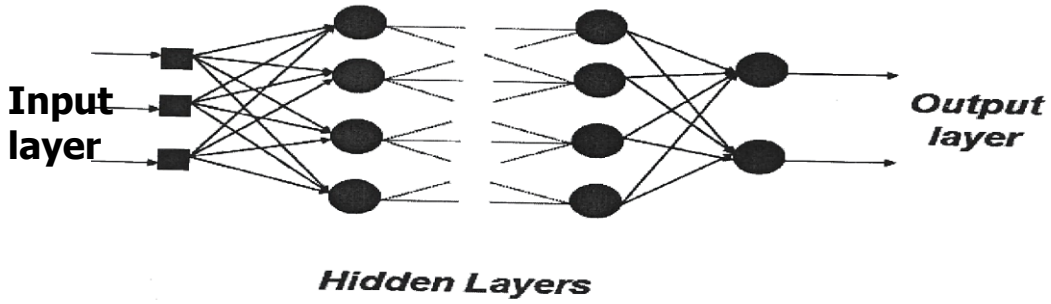

Figure 1: Neural Network Architecture

Ravisankar *et al.* (2014) developed a series of neural networks to predict the influence of welding speed and power on residual stress during gas tungsten arc welding (GTAW) of thin sections with constant heat input. They found that the neural network approach out-performed traditional regression techniques. Taguchi method and ANN were used by Saravanan and Senthilkumar (2015) for predicting wear rate and coefficient of friction for rice husk ash reinforced Al-Si alloy. The results of Taguchi method were used to train the ANN model with the following input parameters: applied load, sliding speed, particle size and weight percentage of reinforcement. The composite was produced by stir casting method and its tribological behaviour was tested on pin-on-disc tribometer in dry sliding conditions. The authors concluded that the developed ANN model can predict wear rate and coefficient of friction up to 95 % accuracy, thus the time consuming and costly experimental process can be avoided. Haque and Sudhakar (2000) developed a neural network model used for predicting the number and depth of pits in heat exchangers. The evolution of the pit depth and the number of pits were effectively modeled and demonstrated a good comparison of the experimental results.

Extreme learning machine (ELM) is a new Artificial Intelligence (AI) learning theory that is capable of learning without iteratively tuning hidden neurons is general architectures (Cao, Lin & Huang 2010). ELM not only proves the existence of the networks but also provides learning solution. The entire hidden node parameters can be randomly generated without training data. This recent innovative data-driven tool makes use of an updated single layer feed forward network (SLFN) algorithm to offer a closed form solution with respect to the output weight via a least squares solution (Ding, Xu & Nie 2014) . This is achieved after resolving the hidden layer weights and biases generated from a continuous probability distribution function instead of utilizing an iterative solution that is being used in artificial neural network model which operates on the feed-forward principle. The time efficiency of the

ELM at resolving regression or classification issues is one of its main distinctive features. This feature is beneficial because the weights and biases which are hidden in the neurons are randomized, while the unique least-square solution of the output can be solved using the Moore-Penrose inverse function.

Because traditional neural networks have had wide uses in system prediction and modelling, ELM also has great potential in the development of accurate and efficient models for these applications. Xu et al. (2013) proposed an ELM based predictor that can be used in the actual frequency stability assessment of power systems. The predictor's inputs are the power system operational parameters, while the output is set as the frequency stability margin. This margin measures the power system's stability degree, subject to a contingency. ELM was also utilized for electricity price forecasting (Cheng & Ou 2011) and temperature predication of molten steel (Tian & Mao 2010). Based on past literature, we can witness its successful applications in control system design, text analysis, chemical process monitor, mechanical properties prediction, clustering and ranking.

Mechanical properties of materials are one of the main factors that determine their applications and should be taken into account during the design and manufacturing of different products. Although successful progress has been achieved in the development of better welding techniques that minimize heat input and residual stresses, considerable effort is still required to develop efficient and cost-effective methods by selecting appropriate input parameters that gives better mechanical properties of weldments. Selection of appropriate current, voltage and welding speed for a given material is essential in obtaining a quality weld (Gery, Long & Maropoulos 2005).
The application of intelligent modelling techniques ANN and ELM in the prediction of mechanical properties of weldments with up to 95 % accuracy saves time and costly experimental process. Knowledge of material properties like tensile strength, hardness, residual stress, and texture as well as phase composition is essential for the later usage of metal parts as they have a direct influence on the capacity to resist loads and other mechanical and physical strains.

Hence, this research focused on optimization and intelligence modelling of tensile strength response of mild steel plate weldments obtained using gas tungsten arc welding process. Specifically, the objectives of this research are: to statistically design experiment for evaluation of welding variables and responses, to determine the effects of welding variables on the tensile strength response of mild steel plate weldments, to develop intelligent models of welding variables and to compare the capabilities of the intelligent models in the prediction of tensile strength response.

2.0 Material and methods

2.1 Material Used

The principal material used in this research is AISI 1018 mild steel plate. Steel is made up of carbon and iron, with much more iron than carbon. Mild steel is one of the most commonly used construction materials because it is very strong and can be made from readily available natural materials. It is known as mild steel because of its relatively low carbon content. Mild steel is very strong due to the low amount of carbon it contains. As opposed to higher carbon steels, mild steel is quite malleable even when cold and has high resistance to breakage. This means that it has high tensile and impact strength. Higher carbon steels usually shatter or crack under stress, while mild steel bends or deforms. Mild steel is especially desirable for construction due to its weldability and machinability. It can be instantly welded by all the conventional welding processes.

2.1.1 Design **of Experiment (DOE): Taguchi Approach**

The modern day approach to find the optimal output over a set of given inputs can be easily carried out by the use of Taguchi method rather than using any other conventional method. The Taguchi method emphasizes the selection of the most optimal solution over the set of given inputs with a reduced cost and increased quality. The optimal solution so obtained is least affected by any outside disturbances like the noise or any other environmental conditions (Rao *et al*, 2008). This method has a wide scope of use varying from the agricultural field to medical field and various fields of engineering and sciences. In the field of Science and engineering, it is used for obtaining optimal results based on the various engineering inputs.

Okafor, Ihueze and Nwigbo (2013) viewed Taguchi robust design as a method of designing experiments in order to investigate how different parameters affect the mean and variance of a process performance characteristic that define how well the process is functioning. The Taguchi method emphasizes the use of loss function, which is the deviation from the desired value of the quality characteristics. Based on loss function, the Signal-to-Noise ratio for each experimental set is evaluated and accordingly the optimal results are derived. The signal-to -noise ratio

measures the sensitivity of the quality investigated to those uncontrollable factors (error) in the experiment. S/N ratio is based upon the larger-the-better criterion for tensile strength response which is calculated using equation 1.

$$\frac{S}{N} = -10log\frac{1}{n}\left(\sum\frac{1}{y_i{}^2}\right) \quad (1)$$

Where n = number of measurements,
y_i = response value for each measurement.

In order to optimize the tensile strength response, four process parameters (current I, voltage V, welding speed S and plate thickness t) were considered. Equally spaced three levels within the operating range of the process parameters were selected as presented in table 1. Based on Taguchi method, an L_9 (3^4) Orthogonal Array (OA) which has nine different experiments was conducted and the result is shown in table 3.

Table 1: Process parameters, Codes, and Level values

Process Parameter	Code	Levels		
		1	2	3
Welding Current (A)	I	100	130	160
Welding Voltage (V)	V	24	28	32
Welding Speed (mm/min)	S	90	120	150
Plate Thickness (mm)	t	6	8	10

2.1.1.1 Sample Production

For each weldment, two plates of dimension 300×120×10mm, 300x120x8mm, and 300x120x6mm in each case were cut and welded to make a weld specimen plate of 300×240×10mm, 300×240×8mm, and 300×240×6mm respectively with a 300 mm weld length. Prior to welding, the plates were cleaned from water, dust and oil to enable proper deposition of electrodes. 60^o V-groove was cut by abrasive cutting on one side of the plates and the plates were tack-welded at both ends in order to eliminate distortion during welding. All necessary precautions were taken to eliminate welding defects. The 60^o V-groove butt joint was made employing symmetric welding sequence as shown in figure 2. Table 2 show the welding consumables and machine settings used during welding.

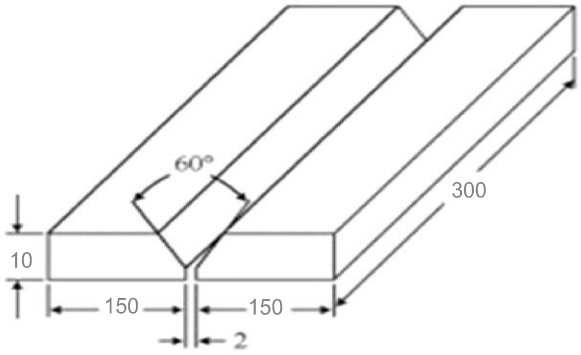

Figure 2: Plate set-up prior to welding

Table 2: GTAW Parameters

S/N	Parameter	6mm plate	8mm plate	10mm plate
1	Electrode type	2%Thoriated W (red) 2.0mm	2%Thoriated W (red) 2.5mm	2%Thoriated W (red) 3.0mm
2	Filler rod	Mild steel 2.0mm	Mild steel 2.5mm	Mild steel 3.0mm
3	Included angle	60^o	60^o	60^o
4	Root face	1.0mm	1.5mm	2.0mm
5	Root gap	1.0mm	1.2mm	1.5mm
6	Gas flow rate	5l/min	7.5l/min	10l/min
7	Current (A)	100, 130, 160	100, 130, 160	100, 130, 160
8	Voltage (V)	24, 28, 32	24, 28, 32	24, 28, 32
9	Number of runs	3	3	3
10	Shielding gas	Helium	Helium	Helium

2.2 Tensile Test

Tensile testing is a fundamental materials science test in which a sample is subjected to a controlled tension until failure. Properties that are directly measured through a tensile test are ultimate tensile strength, breaking strength, maximum elongation and reduction in area. From these measurements the following properties can also be determined: Young's modulus, Poisson's ratio, yield strength, and strain-hardening characteristics. Uniaxial tensile testing is the most commonly used method for obtaining the mechanical characteristics of isotropic materials; hence it was employed in this research. The tensile test on the weldments was conducted as per ASTM Standard E8. Ametek EZ 250 Digital Compression/Tension Tester was used for conducting the tensile test. Three samples were tested in each case and the average value was recorded. Tensile strength was calculated using equation (2).

$$\sigma_t = \frac{F}{wt} \quad (2)$$

Where σ_t is the ultimate tensile strength, F is the peak force, w is the width of the sample, and t is the thickness.

3.0 Results and Discussions

Table 3: Tensile Strength Response for GTAW

S/N	Input Parameters				Tensile Strength (MPa)
	Current (I) A	Voltage (V) V	Welding Speed (S) mm/min	Plate Thickness (t) mm	
1	100	24	90	6	396.5
2	100	28	120	8	382.4
3	100	32	150	10	378.5
4	130	24	120	10	394.6
5	130	28	150	6	383.6
6	130	32	90	8	426.5
7	160	24	150	8	392.8
8	160	28	90	10	422.8
9	160	32	120	6	432.6

3.1 Taguchi Analysis for Tensile Response

Table 4: Response Table for Signal to Noise Ratio

Level	Current (A)	Voltage (V)	Welding Speed (mm/min)	Plate Thickness (mm)
1	51.73	51.92	52.36	52.12
2	52.07	51.95	52.10	52.04
3	52.38	52.29	51.71	52.00
Delta	0.65	0.37	0.65	0.12
Rank	2	3	1	4

Table 5: Response Table for Means

Level	Current (A)	Voltage (V)	Welding Speed (mm/min)	Plate Thickness (mm)
1	385.8	394.6	415.3	404.2
2	401.6	396.3	403.2	400.6
3	416.1	412.5	385.0	398.6
Delta	30.3	17.9	30.3	5.6
Rank	2	3	1	4

Table 6: Analysis of Variance for SN Ratio

Source	DF	Seq SS	Adj SS	Adj MS	F	P
Current (A)	2	0.63510	0.635097	0.317549	0.08	0.003
Voltage (V)	2	0.25566	0.25656	0.127828	0.02	0.002
Welding Speed (mm/min)	2	0.65075	0.650752	0.325376	0.13	0.010
Plate Thickness (mm)	2	0.02188	0.021878	0.010939	0.00	0.000
Residual Error	0	0.00000				
Total	8	1.56338				

S = 0.4426 R^2 = 92.8% R^2 (Adj) = 36.2%

Table 7: Analysis of Variance for Means

Source	DF	Seq SS	Adj SS	Adj MS	F	P
Current (A)	2	1374.91	1374.91	687.454	12.42	0.312
Voltage (V)	2	587.68	587.68	293.841	7.38	0.104
Welding Speed (mm/min)	2	1396.15	1768.45	698.074	13.35	0.422
Plate Thickness (mm)	2	48.54	48.54	24.271	2.65	0.105
Residual Error	0	0.00				
Total	8	3407.28				

S =1 5.8486 R^2 = 92.4% R^2 (Adj) = 36.0%

The estimated model for S/N ratio is obtained as:

$$y = 52.0559 - 0.3304I + 0.0104I - 0.1321V - 0.1057V + 0.3060S + 0.0425S + 0.0654t - 0.0119t \quad (3)$$

The estimated model for Means is obtained as:

$$y = 401.144 - 15.344I + 0.422I - 6.511V - 4.878V + 14.122S + 2.056S + 3.089t - 0.578t \quad (4)$$

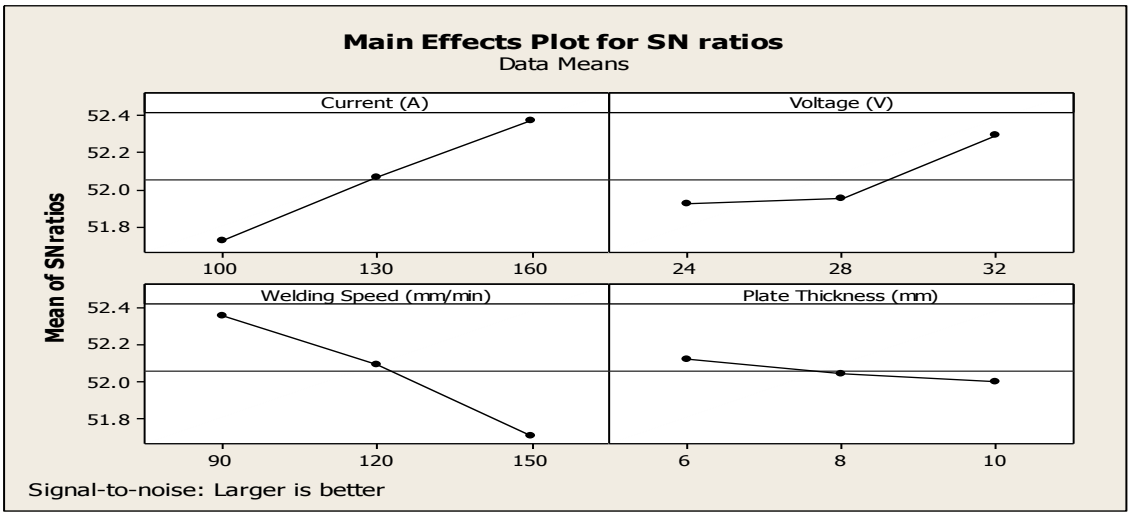

Figure 3: Main Effects Plot for SN Ratio

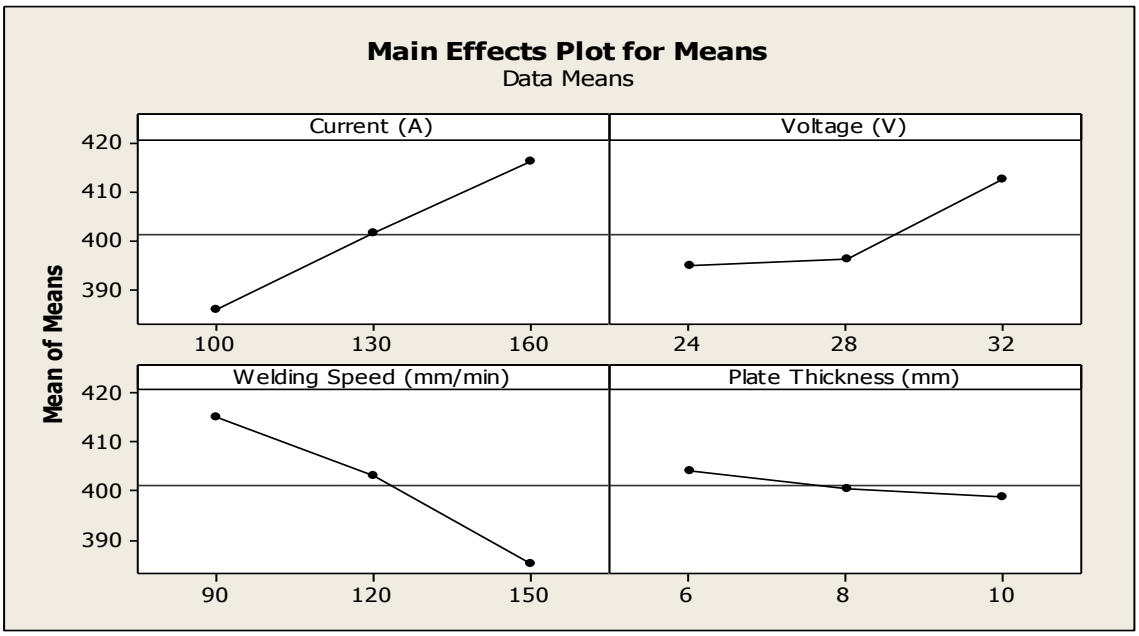

Figure 4: Main Effects Plot for Means

3.1.1 Interpreting Result of Tensile Strength Response

The response tables for signal-to-noise ratio and means for levels of each factor are shown in table 4 and table 5. The ranks in these response tables indicate that welding speed has the greatest influence on tensile response of mild steel plate weldments obtained using gas tungsten arc welding process. This was followed by welding current, welding voltage and plate thickness respectively. In the analysis of variance, the coefficient of determination (R^2) at this point was 92.8% and 92.4% for S/N ratio and mean respectively. This indicates that the linear models of S/N ratio and mean were able to show 92.8% and 92.4% of the variation observed in the dependent variable as captured by the explanatory variables in the linear regression model. These models were completely linear; they did not show interaction effects of the variables.

The main effects plots for S/N ratio and that of means (Figs. 3 and 4) respectively indicate the same outcome of optimum. They show that the optimal tensile strength for gas tungsten arc welding was achieved at a welding current

of 160A, welding voltage of 32V, welding speed of 120mm/min and plate thickness of 6mm. The main effect plots, ranks of factors, values of sum of squares from ANOVA tables are all in conformity with coefficients of the linear models produced for this response. The absolute value of these coefficients shows the importance of each factor to this response; hence, welding speed remains the most significant factor. Based on equations (3) and (4), the optimal tensile strength was obtained as 434.2MPa and 428.6MPa for S/N ratio and for means respectively.

3.2 Intelligence Modelling

The machine learning algorithms applied in this research are artificial neural networks (ANN) and extreme learning machine (ELM) which are both feed-forward neural networks. The ANN and ELM model simulations were carried out in MATLAB 2018a environment at three different hidden neural nodes of 10, 20 and 30 neurons for the thirty (30) experimental runs. The optimum ELM model was determined using the Sigmiod hidden transfer function while the optimum ANN model was determined using Levenberg-Marquart back propagation training algorithm.

The original dataset was split into training, cross-validation and test data sets, where;

- 70% of the exemplars were presented to the network for training.
- 15% of the exemplars concurrent with the training set were used for cross validation.
- 15% of the exemplars were used for testing the trained network.

The following termination criteria were used to determine convergence of the training algorithm:

- Number of runs before termination.
- Maximum number of runs.
- Non-improvement of cross-validation error with training.
- Increase in the cross-validation error with training.

Furthermore, a performance comparison in terms of estimation capacity was conducted between the two models to show their potential in predicting the response.

3.2.1 Score Metrics for ANN and ELM Models

To validate and compare the results from ANN and ELM models, the following score metrics were statistically evaluated. They are; Mean Square Error (MSE), Root Mean Square Error (RMSE), Mean Absolute Deviation (MAD), Mean Absolute Percentage Error (MAPE), Tracking Signal (TS) (Narasimhan, Mcleavey and Billington 1995; Vonderembse & White 1991) and Coefficient of Determination (R^2) (Thorstom 2017). These score metrics are expressed as follows;

$$MSE = \frac{1}{N}\sum_{i=1}^{n}(R_{Pi} - R_{Ti})^2 \quad (5)$$

$$RMSE = \sqrt{\frac{1}{N}\sum_{i=1}^{n}(R_{Pi} - R_{Ti})^2} \quad (6)$$

$$MAD = \frac{1}{N}\sum_{i=i}^{n}|(R_{Ti} - R_{Pi})| \quad (7)$$

$$MAPE = \frac{\sum(|R_T - R_P|/R_T)*100}{N} \quad (8)$$

$$TS = \frac{\sum\frac{R_{Ti} - R_{Pi}}{R_{Ti}}}{\frac{1}{N}\sum_{i=1}^{n}|(R_{Ti} - R_{Pi})|} \quad (9)$$

$$R^2 = 1 - \frac{\sum_{i=0}^{n_{samples}\ -1}(R_{Ti} - R_{Pi})^2}{\sum_{i=0}^{n_{samples}\ -1}(R_{Ti} - \bar{R})^2} \quad (10)$$

where R_{Pi} and R_{Ti} are the predicted and the targeted responses.

3.2.2 ANN and ELM Prediction Results at 10, 20 and 30 Nodes

The ANN and ELM simulation results alongside the experimental results at 10 nodes, 20 nodes and 30 nodes are presented in Tables 8 for tensile strength response.

Table 8: Tensile Strength Prediction at 10, 20 and 30Nodes

Experimental	ANN			ELM		
	10 Nodes	20 Nodes	30 Nodes	10 Nodes	20 Nodes	30 Nodes
383.6	453.06663	429.02375	413.38619	403.68655	395.16142	386.35216
422.8	459.49173	437.87816	427.8426	437.0649	435.20172	460.04088
396.5	396.6316	441.92961	412.43954	403.17928	398.18938	436.29263
392.8	448.61005	421.09872	394.56061	420.94148	400.59183	410.77693
382.4	383.41517	406.46415	393.88381	414.5933	395.96078	416.799

3.2.3 ANN and ELM Prediction Comparison of Tensile Strength at 10, 20 and 30 Nodes

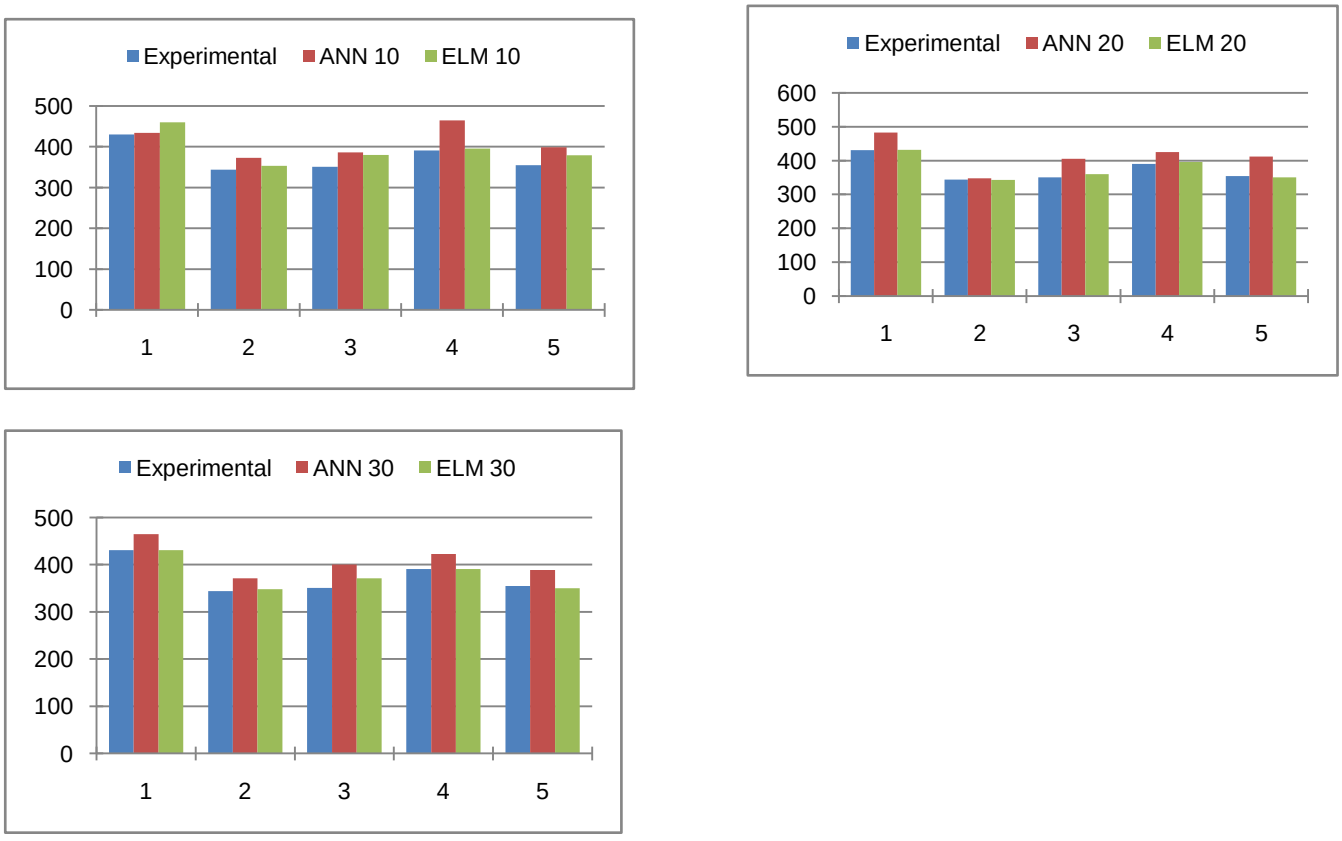

Figure 5: ANN and ELM Prediction Comparison of Tensile Strength at 10, 20 and 30 Nodes

3.2.4 ANN and ELM Scatter Plots for Tensile Strength Response at 10, 20 and 30 Nodes

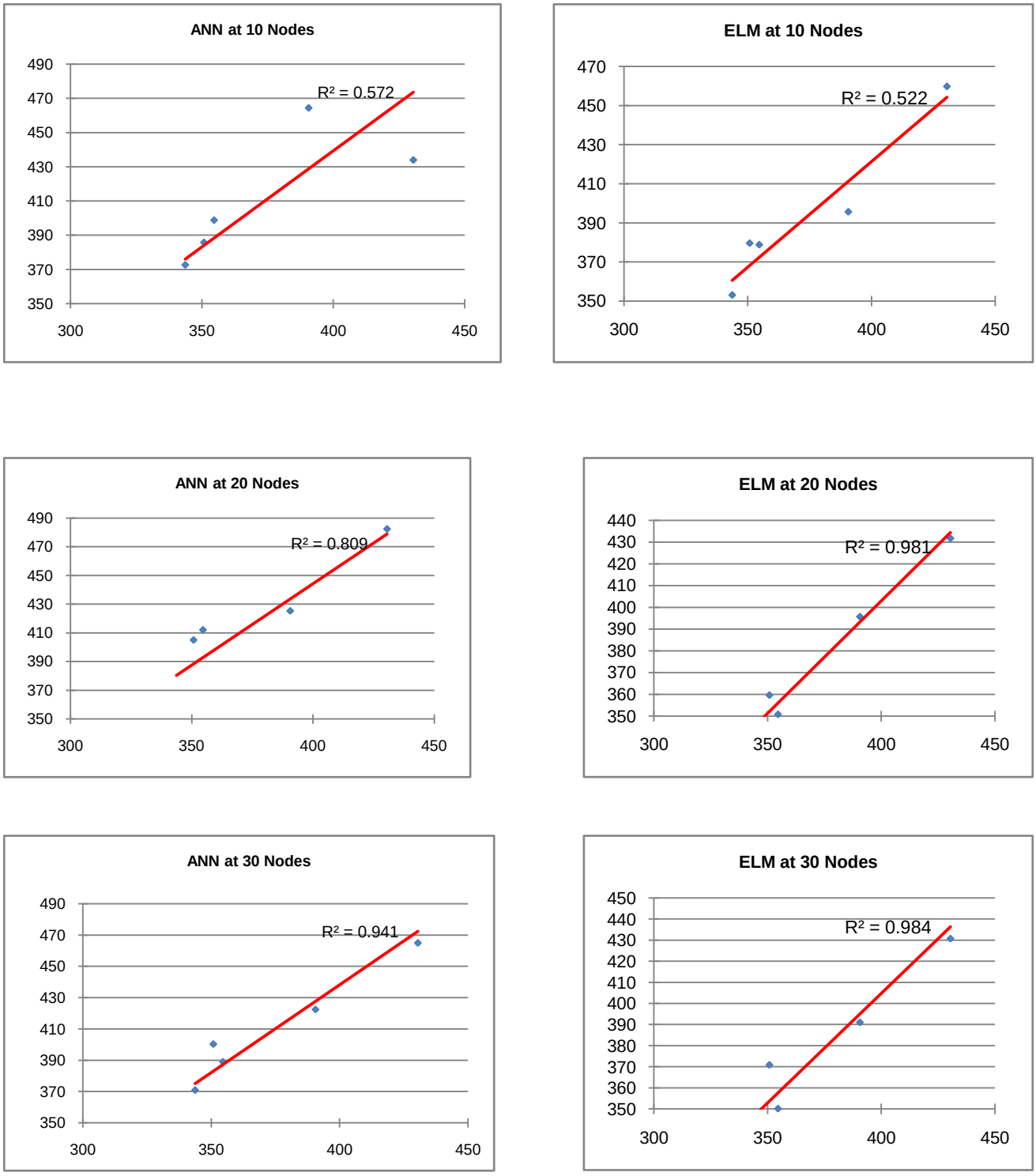

Figure 6: ANN and ELM Scatter Plots for Tensile Strength Response at 10, 20 and 30 Nodes

3.2.5 Performance Metrics for Tensile Strength at 10, 20 and 30 Nodes

The performance metrics for tensile strength at 10, 20 and 30 nodes is shown in table 9 by applying equations (5) to (10).

Table 9: Performance Metrics for Tensile Strength at 10, 20 and 30 Nodes

Metrics	ANN			ELM		
	10 Nodes	20 Nodes	30 Nodes	10 Nodes	20 Nodes	30 Nodes
MAD	37.09878	40.55069	35.51372	19.30732	3.91356	5.83969
MAPE	10.11712	10.77945	9.58555	5.16242	1.07217	1.66254
TS	-5	-5	-5	-5	-2.69233	-3.49202
R2	0.57161	0.80862	0.94129	0.52242	0.98133	0.98369
Time (S)	0.15784	0.08985	1.00246	0.00285	0.00089	0.00985
MSE	1897.94134	2031.65741	1317.56434	475.91181	23.87675	88.09618
RMSE	43.56537	45.07391	36.29827	21.8154	4.88638	9.38596

3.2.6 Discussion of ANN and ELM Results

The tensile strength from the experimental data represents the target (expected) value while the output is the predicted value (response). The model was trained as the output neuron value was adjusted from 10 to 30 in the regression mode. The ELM model was verified against the ANN model which is one of the very popular machine learning black boxes. The ANN and ELM simulation results at 10 nodes, 20 nodes and 30 nodes alongside the experimental results are presented in Table 8. It can be seen from the table that the number of epochs and consequently the time needed for ANN and ELM modeling reduced with rise in the number of nodes. It is also seen from R^2 values and correlation that accuracy of ANN and ELM modeling improved with rise in number of nodes. This means that from both stand points of speed and accuracy, it is better to use higher number of nodes and lesser number of iterations than to use lower number of nodes and higher number of iterations.

Figure 5 show the graphical representation of the predicted values for tensile response at 10, 20 and 30 nodes for both ANN and ELM models. It can be observed from the graphs that at node 30, ELM was the same as the expected values at all the measured points. The advantages of the ELM over the classical ANN model are evident. For example, in accordance with the basic theory of ELM, randomly initiated hidden neurons are fixed, and they do not need iterative tuning process with free parameters or connections between hidden and output layer. Consequently, ELM is remarkably efficient to reach a global optimum, following universal approximation capability of single layer feed-forward network. With suitable activation functions, ELM can attain optimal generalization bounds of traditional feed forward neural networks in which all parameters are learned. This is a distinct advantage of the ELM model in terms of the efficiency and generalization performance over traditional learning algorithm such as ANN as revealed in this research.

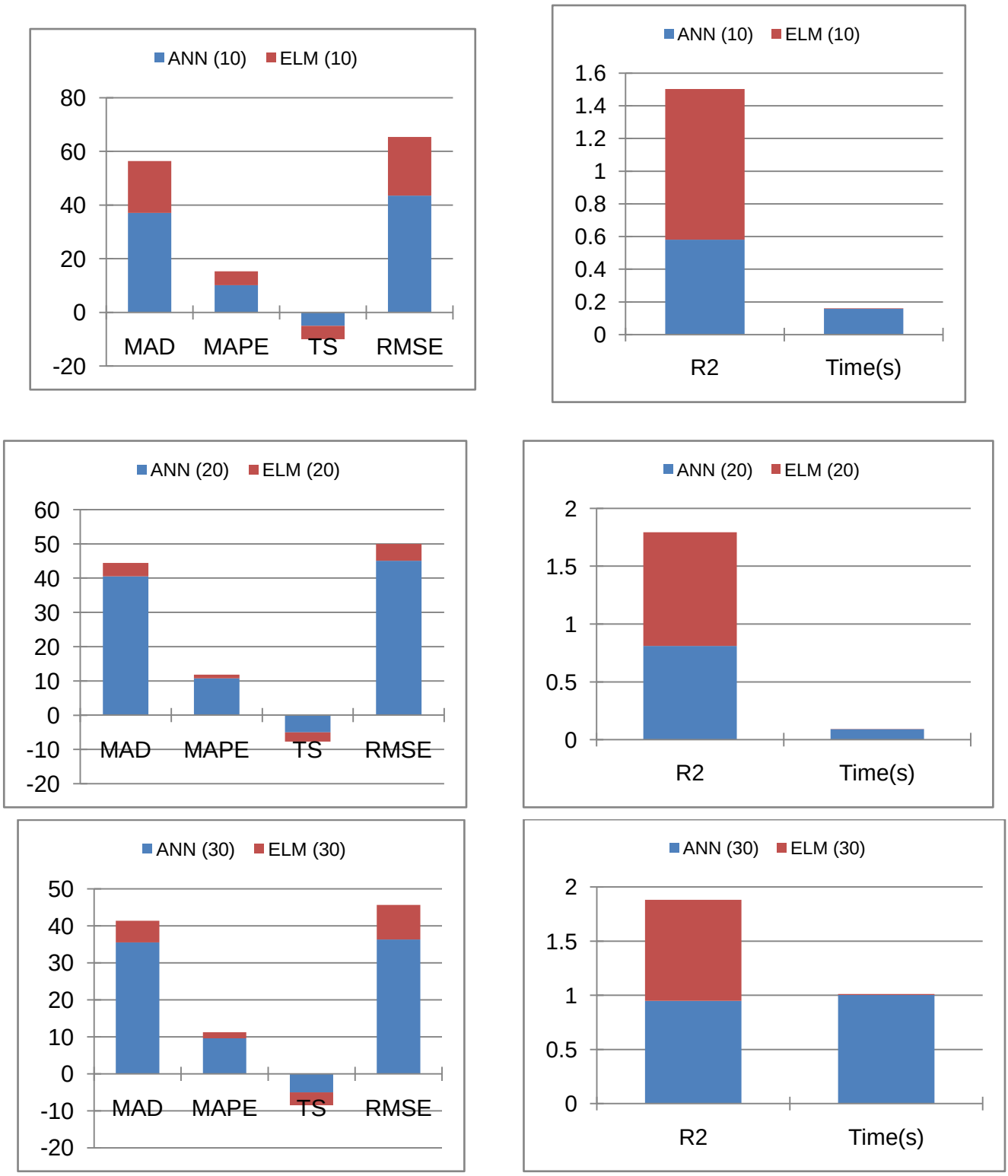

Figure 7: Performance Metrics for Tensile Strength at 10, 20 and 30 Nodes

3.2.7 Discussion of ANN and ELM Scatter Plots

The scatter plots of the predicted values at 10, 20 and 30 nodes are shown in figure 6. From the scatter plots of the predicted response, the highest degree of clusters at the linear regression line is clearly observed on the ELM model. This was specifically pronounced for the ELM model at 30 neural nodes. This particular statistical correlation of targeted and predicted responses at optimum of 30 nodes has a coefficient of determination (R^2) value of 98.4% for ELM, 94.1% for ANN and 92.8% for Taguchi robust design. This result shows that ELM has better prediction capability compared to ANN.

3.2.8 Discussion of Model Performance

Table 9 shows the performance metrics of ANN and ELM. The performances of the models were considered using results gotten from statistical metrics of equations 6 to 11. They are: Mean Square Error (MSE), Root Mean Square Error (RMSE), Mean Absolute Percentage Error (MAPE), Mean Absolute Deviation (MAD), Tracking Signal (TS), and Coefficient of Determination (R^2). Training time for each of the models was also recorded. It is observed that ELM algorithm was simply magnificent in its training time which was much faster than ANN for all neural nodes. At 30 neural nodes, the training time for ELM was 0.009 Seconds while that of ANN was 1.00 Seconds.

The MSE and MAD are statistical approaches used to verify the prediction error. It was found that the MSE, RMSE, MAD and MAPE all improved as the output neuron value increased and fully converged at 30 neural nodes. This means that the higher the number of output neurons, the better the response. While the hidden nodes of ANN can be adjusted, they are not accessible in ELM. The tracking signal (TS) helps to determine if the model is an accurate representation of the real-world variable. It is expected to be theoretically equal to zero. Both ELM and ANN models have tracking signals recorded at sub-zero for all the nodes. This indicates that the models have good tracking signal; hence the models are good.

4.0. Conclusion

At the end of this research, the following conclusions are made:

1. Based on analysis of the experimental results using Taguchi method, ANN and ELM algorithms, it can be concluded that all the methods gave reliable results.
2. Taguchi method can be successfully applied to optimize the parameters which influence the tensile response of mild steel plate weldments whereas ANN and ELM models can be used for predicting the response.
3. By comparing the experimental results with those obtained using ANN and ELM models, it can be concluded that the ELM model is more efficient in predicting tensile strength of mild steel plate weldments.

5.0 Recommendation

1. After obtaining experimental results of the mechanical properties of weldments, ANN and ELM models can both be reliably used to predict the mechanical properties. If both models are available, ELM is highly recommended.
2. Examination of the connection between ELM algorithm and Random Forest algorithm should be carried out.

Nomenclature/Abbreviations

AI	Artificial Intelligence
ANN	Artificial Neural Network
ASTM	American Society of Testing and Materials
ELM	Extreme Learning Machine
GTAW	Gas Tungsten Arc Welding
MAD	Mean Absolute Deviation
MAPE	Mean Absolute Percentage Error
ML	Machine Learning
MSE	Mean Square Error
RMSE	Root Mean Square Error
SLFN	Single Layer Feed-forward Neural Network
TS	Tracking Signal

References

American Welding Society. 2004. The metallurgy of steel (4th Ed.), Chicago. *pp. 26–31*. ISBN 9780871708588.

Cao, J., Lin, Z. & Huang, G. B. 2010. Composite function wavelength neural networks with extreme learning machine. *Journal of Neurocomputing*, 73(7), 1405-1416.

Cheng, F. & Ou, T. 2011. Sales forcasting system based on gray Extreme Learning Machine with Taguchi method in retail industry. *Expert Systems with Applications*, 38(3), 1336-1345.

Devaraju, J. D. 2015. An Experimental study on TIG welded joint between Duplex Stainless Steel and 316L Austenitic Stainless Steel. *International Journal of Mechanical Engineering*, ISSN: 2348 – 8360.

Dietterich, T. G. 1990. Machine learning. *Annual Review of Computer Science*, Vol.4, 255-306.

Ding, S., Xu, X. & Nie, R. 2014. Extreme learning machine and its applications. *Neural Computing and Applications*, 5, 14-34.

Gery, D., Long, H. & Maropoulos, P. 2005. Effects of welding speed, energy input and heat source distribution on temperature variations in butt joint welding. *Journal of Materials Processing Technology*, 167, (23), 393-401.

Gurney, K. 1997. *An Introduction to Neural Networks.* London: UCL Press Limited.

Haque, M. E. & Sudhakar, K. V. 2000. Prediction of corrosion fatigue behavior of DP steel through Artificial Neural Network. *International Journal of Fatigue Science*, 23(1), 1-4.

Jain, R. K., 2013. Production Technology. Khanna Publishers (17th edition), New Delhi.

Nasasimhan, J., Mcleavey, Z. & Billington, G. 1995. Composite function wavelength neural networks with extreme learning machine. *Journal of Neurocomputing*, 73(7), 1405-1416.

Okafor, C. E, Ihueze, C. C. & Nwigbo, S.C. 2013. Optimization of hardness strengths response of plantain fibres reinforced polyester matrix composites applying Taguchi robust design. *International Journal of Engineering*, 26(1), 21-38.

Okafor, C. E., Okafor, E. J, and Ikebudu K. O. (2021). Evaluation of machine learning methods in predicting optimum tensile strength of microwave post-cured composite tailored for weight-sensitive applications. *Engineering Science and Technology, an International Journal.* https://doi.org/10.1016/j.jestch.2021.04.004

Rao, R.S., Ganesh, K.C., Shetty, P.S. & Phil, J.H. 2008. The Taguchi methodology as a statistical tool for biotechnological applications: A critical appraisal. *Biotechnology Journal*, 3(4), 510-523.

Ravisankar, A., Velaga, S.K., Rajput, G. & Venugopal, S. 2014. Influence of welding speed and power on residual stress during gas tungsten arc welding (GTAW) of thin sections with constant heat input: a study using numerical simulation and experimental validation. *Journal of Manufacturing Processes*, 16(2), 200–211.

Reed, R. D. & Marks, R. J. 1998. *Neural Smithing: Supervised learning in feed forward Artificial Neural Networks.* Cambridge, MA: MIT Press.

Saravanan, S. D. & Senthilkumar, M. 2015. Prediction of tribological behaviour of rice husk ash reinforced aluminum alloy matrix composites using artificial neural network. *Russian Journal of Non-Ferrous Metals*, 56 (1), 97-106.

Tian, C. & Mao, P. 2010. Prediction of molten steel temperature in steel making process using extreme earning machine. *Journal of Chemical Engineering of Japan*, 47(11), 827-834.

Thorstom, H. 2017. Extreme learning machine and its applications. *Neural Computing and Applications*, 5, 14-34.

Vonderembse, F. & White, T. 1991. Sales forcasting system based on gray Extreme Learning Machine with Taguchi method in retail industry. *Expert Systems with Applications*, 38(3), 1336-1345.

Xu, Y., Dai, Y. Y., Dong, Z. Y., Zhang, R. & Meng, K. 2013. Extreme learning machine-based predictor for real-time frequency stability assessment of electric power systems. *IET Generation, Transmission and Distribution*, 7(4), 391–397.